JPE 12-1-21

http://dx.doi.org/10.6113/JPE.2012.12.1.164

Scaling Factor Design Based Variable Step Size Incremental Resistance Maximum Power Point Tracking for PV Systems

Emad M. Ahmed† and Masahito Shoyama*

†* Graduate School of Information Science and Electrical Engineering, Kyushu University, Fukuoka, Japan

Abstract

Variable step size maximum power point trackers (MPPTs) are widely used in photovoltaic (PV) systems to extract the peak array power which depends on solar irradiation and array temperature. One essential factor which judges system dynamics and steady state performances is the scaling factor (N), which is used to update the controlling equation in the tracking algorithm to determine a new duty cycle. This paper proposes a novel stability study of variable step size incremental resistance maximum power point tracking (INR MPPT). The main contribution of this analysis appears when developing the overall small signal model of the PV system. Therefore, by using linear control theory, the boundary value of the scaling factor can be determined. The theoretical analysis and the design principle of the proposed stability analysis have been validated using MATLAB simulations, and experimentally using a fixed point digital signal processor (TMS320F2808).

Key Words: Incremental resistance (INR), Linearized model, Maximum power point (MPP), Maximum power point tracking (MPPT), Scaling factor (N), Small signal stability, Variable step size

NOMENCLATURE

v_{PV}	Photovoltaic module output voltage (V)
i_{PV}	Photovoltaic module output current (A)
P_{PV}	Photovoltaic module output power (W)
D	Converter duty cycle at the MPP
Δd	Converter duty cycle variation around the MPP
N	Duty cycle scaling factor
V_{mmp}	PV module voltage at the MPP
I_{mpp}	PV module current at the MPP
R_{mpp}	PV module equivalent resistance at MPP
I_L	Steady state inductor current
C_{in}	Converter Input capacitor
L	Boost converter inductor
C_{out}	converter output capacitor
R_L	Load resistance
V_o	load terminal voltage (output voltage)
T	Sampling Time in second
e	Incremental Resistance actuating error around MPP
Δe	Linearized error variation around MPP

Manuscript received May 27, 2011; revised Oct. 31, 2011
Recommended for publication by Associate Editor Woo-Jin Choi.
† Corresponding Author: el-bakoury@ieee.org
Tel: +81-92-802-3704, Fax: +81-92-802-3703, Kyushu University
* Graduate School of Information Science and Electrical Engineering, Kyushu University, Japan

I. INTRODUCTION

The ever-increasing demand for low-cost energy and growing concerns about environmental issues has generated enormous interest in the utilization of non-conventional energy sources such as solar energy [1], [2].

A major challenge in the use of PV is due to its nonlinear current-voltage (I-V) characteristics, which result in a unique MPP on its power voltage curve (P-V). The matter is further complicated by the dependence of these characteristics on solar irradiation and temperature. Therefore, it is essential to continuously track the MPP in order to maximize the output power from a PV system. The subject of MPPT has been studied in different ways in the literature. Examples of fuzzy logic, extremum seeking, neural networks, and pilot cells have been proposed in [3]–[5]. Moreover, the perturb and observe (P&O), and the incremental conductance INC MPPT techniques are widely used, due in large part to their lower cost implementation when compared with other techniques [6].

The main shortcoming of the P&O technique is that, at the steady state, the operating point oscillates around the MPP resulting in the waste of some of the available energy. Several improvements of the P&O algorithms have been proposed in order to reduce the number of oscillations around the MPP in the steady state. However, they slow down the response of the algorithm to changes in atmospheric conditions and they reduce the algorithm efficiency during rapidly changing atmospheric conditions [6]. However the INC MPPT algorithm was designed based on the incremental and the instantaneous

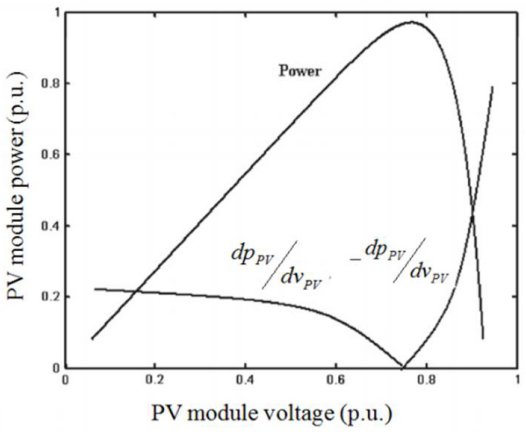

Fig. 1. Schematic diagram of INC-MPPT equipped with DC-DC Boost Converter.

conductance values of a PV array. The derivative of the PV module power P_{PV} is positive before reaching the MPP, zero at the MPP, and negative after passing the MPP, as shown in Fig. 1. The main advantage of INC MPPT is its ability to efficiently track the MPP without a tendency to deviate from the MPP due to rapidly changing atmospheric conditions as is the case with the P&O technique [7].

The INC MPPT algorithm usually uses a fixed step size perturbation to track the maximum power point (MPP). Thus, the tracking speed and accuracy are highly depending on the fixed step size perturbation *(ΔD)*. The power drawn from the PV array with a lager step size contributes to faster dynamics but also exhibits excessive steady state oscillations around the MPP, resulting in a comparatively low efficiency. However, the situation is reversed with a smaller step size [8]. Accordingly, in order to overcome the aforementioned challenge, a variable step size MPPT has to be adopted to address the tradeoff between the dynamics and the steady state oscillations. In the variable step size MPPT schemes, the automatic tuning equation of the variable step size was proposed to be a function of the PV power derivative with respect to the PV voltage, as shown in Fig. 1. The updating variable step size equation has been written as in the form (1) [8].

$$\begin{aligned} D(k) &= D(k-1) \pm N \times \left| \frac{dp_{PV}}{dv_{PV}} \right| \\ &= D(k-1) \pm N \times \left| \frac{p_{PV}(k) - p_{PV}(k-1)}{v_{PV}(k) - v_{PV}(k-1)} \right| \end{aligned} \tag{1}$$

where *D(k),* and *D(k-1)* are the converter duty cycles at instants *K,* and *k-1*, respectively. As can be seen from (1), the scaling factor *N* adjusts the input signal to a proper magnitude prior to determining the subsequent step size. Therefore, it is crucial to design the most appropriate value for the scaling factor *N*, which ensures better dynamic and steady state performances. A bad designing of the scaling factor might lead to undesired performances such as steady state oscillations and a slower dynamic response.

The only method proposed in the literature for designing the scaling factor is in [8]. Although this method can be considered as a simple method for designing the scaling factor, it requires a prior analysis of the system for fixed step size operation. Therefore, this method had neither realized the effect of increasing or decreasing the scaling factor on the system stability and the dynamic performance, nor formalized a closed form or a straight forward approach for designing its value. Furthermore, a bad design of the scaling factor will change the system operation from variable step size mode to fixed step size mode, which consequently reduces the system efficiency.

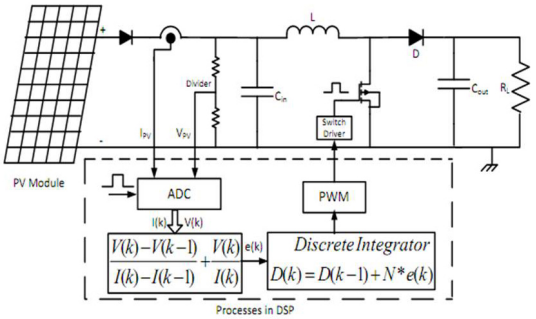

Fig. 2. Schematic diagram of INR-MPPT equipped with DC-DC Boost Converter.

In this paper, in order to design an appropriate value for the scaling factor *N* and to study the overall system stability, the INR MPPT scheme for a PV system has been introduced in part II. System modeling and analysis, which contain the converter small signal model, the INR MPPT error linearization, and the complete small signal model of a PV system, have been presented in part III. Part IV introduces MATLAB simulation results for the proposed small signal strategy with different values of the scaling factors. Moreover, part V presents experimental results conducted in the laboratory with a PV solar panel and a digital signal processor DSP. Finally, part VI presents the overall conclusion of this study.

II. INR-MPPT Scheme for PV System

A schematic diagram of INR MPPT is shown in Fig. 2. The primary rules for the INR MPPT algorithm can be deduced by duality from the INC MPPT as follows: the power curve of the PV module shows that the derivative of the PV module power PPV is positive before reaching the MPP, zero at the MPP, and negative after passing the MPP, as shown in Fig. 3. The derivative of PPV is given in (2), and the resultant equation for the actuating error e is given in (3).

$$\frac{dp_{PV}}{di_{PV}} = \frac{d(v_{PV} \times i_{PV})}{di_{PV}} = \frac{dv_{PV}}{di_{PV}} \times i_{PV} + v_{PV} \tag{2}$$

$$e = \frac{dv_{PV}}{di_{PV}} + \frac{v_{PV}}{i_{PV}} \tag{3}$$

Therefore, tracking the maximum power point MPP requires the updating rule as follow in (4).

$$\begin{cases} 1)\ D(k) = D(k-1) + N \times |e(k)| & e(k) > 0 \\ 2)\ D(k) = D(k-1) & e(k) = 0 \\ 3)\ D(k) = D(k-1) - N \times |e(k)| & e(k) < 0 \end{cases} \tag{4}$$

By examining (4), this equation can be implemented by a simple digital integrator with the error signal *e* considered as its input, and a scaling factor *N* as the integrator gain, as shown in Fig. 2. The function of the scaling factor gain

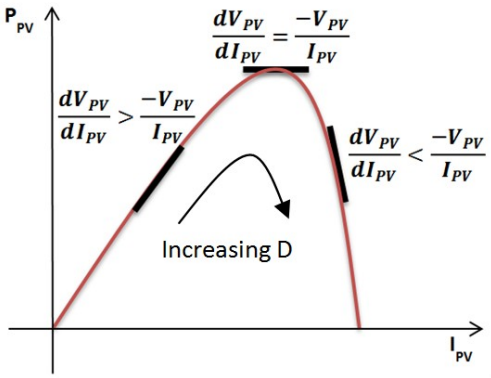

Fig. 3. Incremental Resistance (INR) relation with Instantaneous resistance.

N is to adapt the error signal e to a proper range before the integral compensator. Since the error signal e becomes smaller as the operating point approaches the MPP, an adaptive and smooth tracking can be achieved [9], [10]. In order to design an appropriate scaling factor value N, which ensures a good dynamic performance and stability, a small signal model has to be developed for the overall linearized system around the MPP.

III. System Modeling and Analysis

A straight forward approach for designing an appropriate scaling factor and for studying system stability is developing a linearized model of the overall system around the MPP. The linearization process for the overall system can be divided into two main categories. The first one is developing a converter small signal model with the PV model, and the second one is linearizing the INR actuating error e around the MPP. Both categories will be explained in the following subsections.

A. Converter Small Signal Model.

In order to derive a mall signal model of a boost converter equipped with a PV module around the MPP, the PV module has been replaced with an equivalent resistance R_{mpp} [6]. The state space averaging model of a boost converter equipped with a PV module at the MPP can be deduced using Fig. 4(a) and Fig. 4(b) [11].

The small signal transfer function between the output voltage (Δv_{PV}) as the controlling output and the converter duty cycle (Δd) as the controlling input can be written as:

$$G_{vd}(s) = \frac{\Delta v_{PV}}{\Delta d} = \frac{-(z_1 s + z_2)}{p_1 s^3 + p_2 s^2 + p_3 s + p_4} \quad (5)$$

where

$$z_1 = V_o R_L R_m C_{out}$$

$$z_2 = I_L R_L R_{mpp}(1-D) + V_o$$

$$p_1 = R_{mpp} C_{in} L R_L C_{out}$$

$$p_2 = R_{mpp} C_{in} L + R_L L C_{out}$$

$$p_3 = (1-D)^2 R_L R_{mpp} C_{in}$$

$$p_4 = I_L R_L R_{mpp}(1-D) + V_o$$

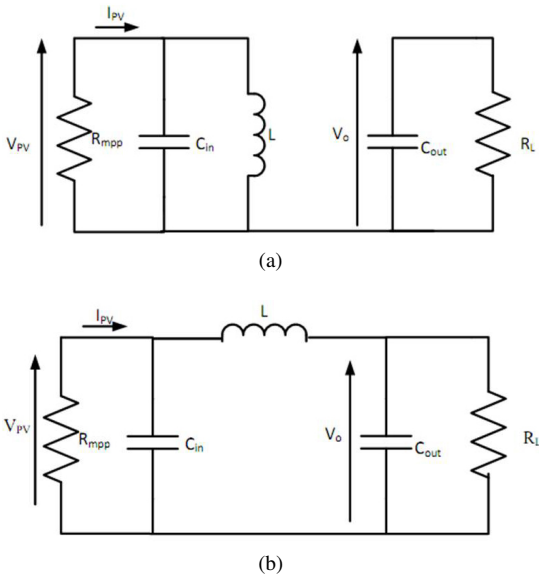

Fig. 4. Converter equivalent circuit with the PV module during. (a) On state. (b) Off state.

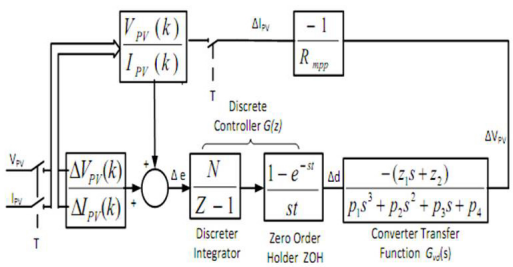

Fig. 5. PSchematic diagram of the PV system equipped with Digital INR MPPT.

Thus the boost converter equipped with the PV module is modeled around the MPP with a third order system containing the effects of the PV parameters (R_{mpp}) and the converter parameters (C_{in}, C_{out}, L, R_L), as shown in (5).

B. Incremental Resistance error Linearization.

A schematic block diagram of a PV system equipped with the digital INR MPPT is shown in Fig. 5. The feed forward loop contains the small signal model of the boost converter $G_{vd}(s)$ and the discrete controller, which consists of the discrete integrator and the zero order holder blocks.

Obviously, the dynamic performance and the system stability are highly depend on the feedback loop which consists of the discrete controller $G(z)$ and the converter transfer function G_{vd} (s). The loop gain can be written as in (6).

$$Loop\,gain(s) = G(s) \times G_{vd}(s) \times \frac{-1}{R_{mpp}} \quad (6)$$

where $G(s)$ represent the continuous transfer function of the discrete controller $G(z)$.

In order to drive the continuous transfer function $G(s)$, the error signal e should be linearized around the MPP. Therefore, a straight line has been drawn tangentially to the IV curve. This line pass through (V_{mpp}, I_{mpp}), and has a slop of (-R_{mmp}), as can be seen in Fig. 6. Thus, the straight line equation can be written here as (7).

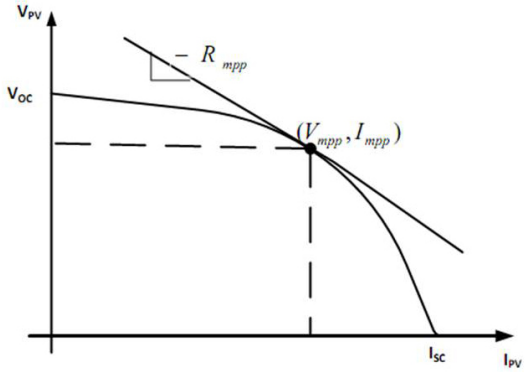

Fig. 6. PV Module Linearization around the MPP.

$$v_{PV} = 2V_{mpp} - i_{PV} \times R_{mpp} \tag{7}$$

Using (7), the actuating error e has been linearized by adapting the Taylor series expansion and retaining only the linear terms as in appendix (A). Therefore, the linearized actuating error variation around the MPP is rewritten like (A6) as:

$$\Rightarrow \Delta e = -\left(\frac{2R_{mpp}}{I_{mpp}}\right)\Delta i_{PV} \tag{8}$$

Therefore by using (8), the transfer function between Δi_{PV} and Δd can be written in the discrete form, as shown in Fig. 5, as:

$$\frac{\Delta d(z)}{\Delta i_{PV}(z)} = -\left[\frac{2R_{mpp}}{I_{mpp}}\right] \times \frac{N}{z-1} \tag{9}$$

Finally, the continuous time expression of the discrete controller is derived by substituting $z = e^{sT}$ into (9), and then multiplying $(1-e^{-sT})/sT$to represent the effect of zero order holder (ZOH) [9]. The final expression is:

$$\frac{\Delta d(s)}{\Delta i_{PV}(s)} = -\left[\frac{2R_{mpp}}{I_{mpp}}\right] \frac{N \times e^{-sT}}{sT} \tag{10}$$

Since the sampling time (T) is very small, the time delay term e^{-sT} can be approximated using the Taylor series expansion as (*1-sT*) and neglecting the higher order terms. Therefore (10) can be re-written as:

$$\frac{\Delta d(s)}{\Delta i_{PV}(s)} = -\left[\frac{2R_{mpp}}{I_{mpp}}\right] \frac{N \times (1-sT)}{sT} \tag{11}$$

The overall small signal model of the linearized INR MPPT can be drawn as in Fig. 7. Using the automatic control theory, the characteristic equation of this system can be derived as:

$$Cheq = 1 + \frac{2N \times R_{mpp}}{I_{mpp}} \times \frac{(1-sT) \times (z_1 s + z_2)}{sT \times (p_1 s^3 + p_2 s^2 + p_3 s + p_4)} \tag{12}$$

where *Cheq* represents the system characteristic equation. As can be seen from (12), the system dynamic stability is highly dependent upon the scaling factor N and the sampling time T. Decreasing the sampling time T tends to increase the system loop gain, which leads to duty cycle overcompensation and hence decreases in system stability. However increasing the sampling time T decreases the system loop gain, which

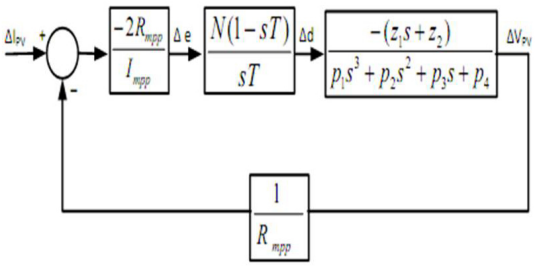

Fig. 7. The closed loop small signal model.

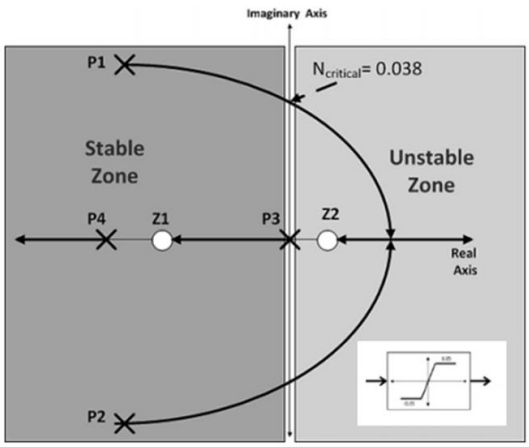

Fig. 8. Root-Locus sketch of the overall system model at MPP with scaling factor (N) variation from 0 to ∞ (P: pole, Z: zero).

decelerates the tracker performance. However, the effect of the scaling factor N has not been studied in the literature.

A root-locus plot of the overall system presented by (12), with the system parameters defined in table 1, is shown in Fig. 8. As can be seen from this plot, increasing the scaling factor N increases the dc loop gain, which reduces the system stability. In order to ensure stable operation, the scaling factor should be designed within the specified limits ($0 < N \leq 0.038$).

IV. Digital Simulation Results

To validate the above analysis, a MATLAB SIMULINK model was established for a PV module equipped with a DC-DC boost converter and a resistive load, as shown in Fig. 2. A small signal model has been established for the PV system under the standard conditions (1000 W/m^2, 25°C). The sampling time T has been selected to be 0.01s [6]. All of the system parameters are shown in table 1 [12]. By drawing the root-locus of this system with the defined parameters, the boundary values of the scaling factor N are determined as ($0 < N \leq 0.038$).

In order to investigate the correctness of the proposed small signal model for INR MPPT, the performance of a PV system has been checked with different values of the scaling factor N. The simulations are configured under exactly the same conditions. Since selecting a scaling factor N outside the stable boundary will lead to undesirable conditions, a limiter has been added to limit the divergence in the duty cycle variation (Δd). The upper and lower values of this limiter have been selected as $\pm\Delta d$=$\pm$0.05, as shown in Fig. 9.

TABLE I
PV SYSTEM PARAMETERS (1000 W/M^2, 25°C)

V_{OC} (open circuit voltage)	21.2 V
V_{mpp} (voltage at max power)	17 V
I_{SC} (Short circuit current)	3.25 A
I_{mpp} (current at max power	3.01A
P_{MPP} (maximum power)	51 W
C_{in} (input capacitor)	47uF
L (Inductor)	1 mH
C_{out} (output capacitor)	47uF
F_s (switching frequency)	30 kHz
R_L (load resistance)	40 Ω

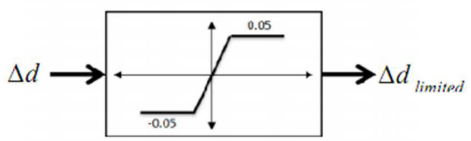

Fig. 9. Duty cycle variation limiter.

Three scaling factors have been selected. Two of the values are in the stability zone (*N= 0.004, N= 0.01*) and the other is in the marginal or instability zone (*N= 0.04*).

Fig. 10(a) shows the PV module output power when there is a sudden change in the irradiation density from 1000 W/m^{2}to 600 W/m^2 at instant 1 sec and then a change back again from 600 W/m^2 to 1000 W/m^2 at instant 2 sec. The corresponding converter duty cycle is shown in Fig. 10(b). It can be seen from this figure that the steady state response is free from any oscillation around the MPP and that it has a fast dynamic response ($\sim$ 0.1 sec). Fig. 10(b) shows the converter duty cycle while tracking the peak power. On the other hand, Fig. 10(c) and Fig. 10(e) show the dynamic response of the PV system at N equals 0.01 and 0.04, respectively.

As can be seen from Fig. 10(c), as the scaling factor increases and gets very close to the boundary values, the dynamic response of the PV module starts to exhibit steady state oscillations around the MPP. As a result, a small amount of the available power is wasted. However, the dynamic response does not have a large change from the previous state (at *N= 0.004*). This can also be noticed in the converter duty cycle in Fig. 10d. As the scaling factor increases and goes outside the stability zone, the dynamic response changes to work as a fixed step size operation which is characterized by a lower efficiency than the variable step size. Thus, the variation in the duty cycle changes to have a fixed step size (0.05). These can be seen in Fig. 10(e) and Fig. 10(f).

By inspecting the previous simulation results, it can be concluded that selecting a scaling factor outside the stability zone ($N > 0.038$), leads to overcompensation in the duty cycle.

Thus, the duty cycle variations deviate from the stability zone. As a result, the added limiter becomes necessary for limiting this deviation and changing the operation to fixed step size. As a consequent, the dynamic operation changes into a fixed step size operation with a step size equal to the limited value. However, selecting a scaling factor in the stability zone ensures a good dynamic response as well as a good steady state response. Therefore, these simulation results ensure the feasibility and the validity of the proposed stability analysis in determining the boundary values of the variable step size scaling factor.

V. EXPERIMENTAL RESULTS

The investigation of the proposed small signal stability analysis has been also evaluated by experiment. A PV power simulator (Agilent E4360) is used as the PV module. The PV simulator is programmed to simulate a PV curve for the simulated model, which is shown in table 1. This was done by entering the corresponding values V_{OC}, V_{mpp}, I_{mpp}, and I_{sc}. The INR MPPT algorithm was configured on a fixed point 12 bit digital signal processor (DSP TMS320F2808) using the MATLAB SIMULINK toolboxes. The main program was developed in the MATLAB SIMULINK environment.

The target is programmed using code composer 3.3. A duty cycle variation limiter with $\pm\Delta D_{max}$=$\pm$0.05 is introduced. The start waveforms of the output power are shown in Fig. 11. Figure 11 shows the dynamic response of the PV system employed by the INR MPPT with different scaling factors. The dynamic response of the fixed step size INR MPPT is shown in Fig. 11(a). Although the tracker has a fast transient response (10 cycles – 0.1s), the tracker cannot pick up the maximum power (P_{max}= 51 W) due to its operation with a fixed step size. The average amount of power extracted is equal to 44.6 W. Fig. 11(b), Fig. 11(c), and Fig. 11(d) show the dynamic response of the PV module with different the scaling factors 0.002, 0.01, and 0.04, respectively. As can be seen, a lower scaling factor ensures a better steady state performance without exhibiting any steady state oscillations around the MPP, as shown in Fig. 11(b). However, a lower scaling factor slows down the transient response to 29 cycles (0.29 s).

Furthermore, by increasing the value of the scaling factor, the transient response starts to have a fast dynamic response (10 cycles- 0.1s) and a higher efficiency than the fixed step size operation, as shown in Fig, 11c, and Fig. 11(d). On the other hand, the steady state performance starts to exhibit steady state oscillations around the MPP, which reduces the average amount of extracted power. Moreover, it is obvious, that increasing the scaling factor beyond the stability zone, indicated in Fig. 8, will lead to variable step overcompensation. Therefore, the variable step size operation has the tendency to operate as a fixed step size, as can be seen in Fig. 11(d).

To investigate the performance of the variable step size with different irradiation conditions, a scaling factor (N= 0.002) has been selected. Fig, 12(a) shows the dynamic response of the PV module with fixed step size INR MPPT. The dynamic performance of the PV system exhibits large oscillations around the MPP. While the variable step size introduces a better dynamic performance than the fixed step size, these appear with the higher power generated: at 1000 W/m^2 the generated power with a variable step size is 48.8 W and with a fixed step size it is 44.6 W. Also, at 600 W/m^2, the generated power with a variable step size is 28.8 W and with a fixed step size it is 27.6 W.

It is clear from the experimental results, that the dynamic performance is highly affected by the scaling factor. A bad design of the scaling factor leads to a worse dynamic response. However, selecting an appropriate scaling factor ensures high efficiency tracking and acceptable transient and steady state performances.

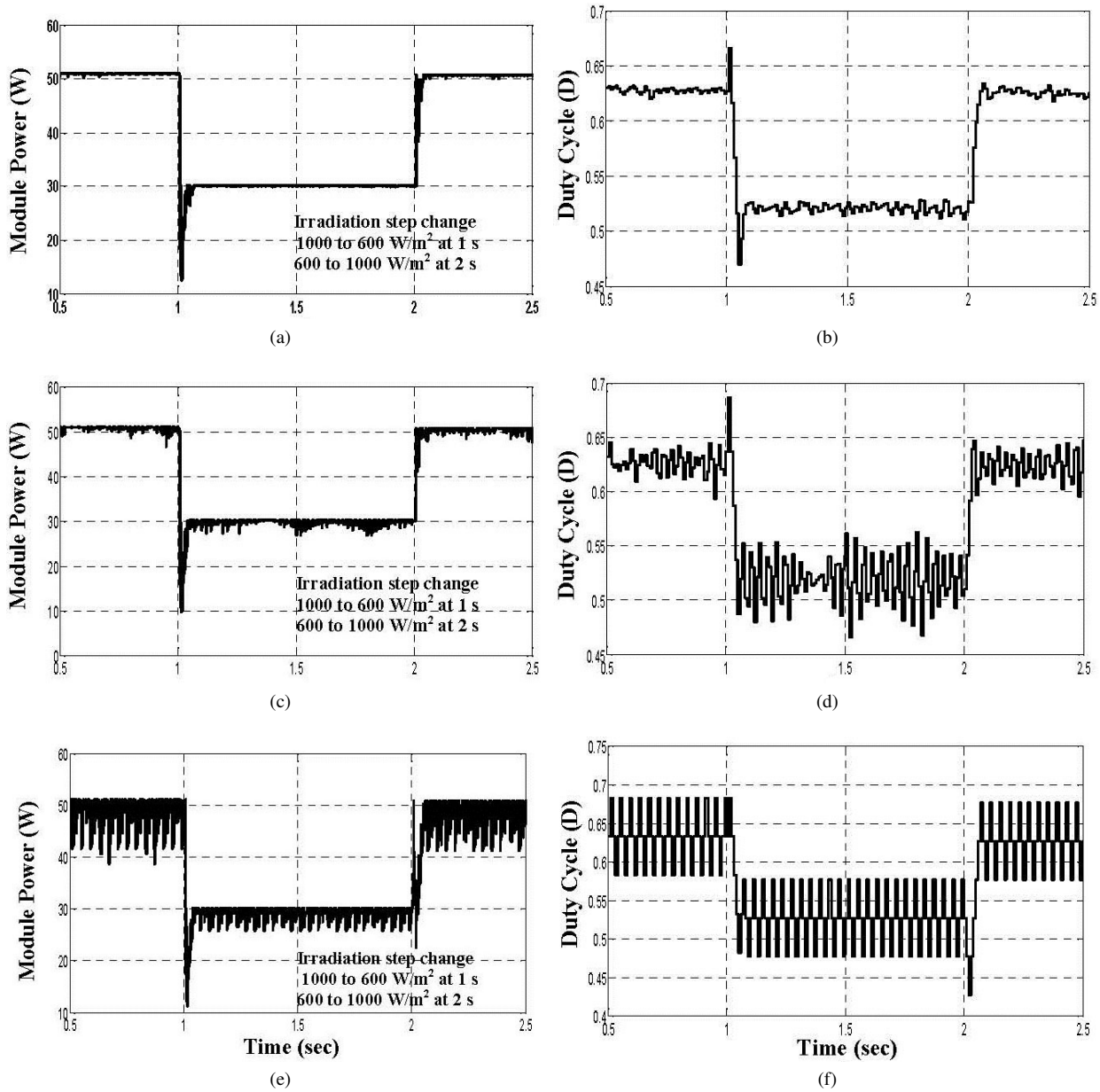

Fig. 10. PV array output power and the corresponding duty cycle due to irradiation step change with (a),(b) $N = 0.004 << 0.038$. (c),(d) $N = 0.01 < 0.038$. (e),(f) $N = 0.04 > 0.038$.

VI. Conclusion

A new stability analysis for INR MPPT has been presented in this paper. The proposed analysis depends on developing an overall small signal model of the PV system around the MPP. The small signal model of the PV system consists of the PV module, the boost converter, and the discrete INR MPPT. Using the root locus technique, or any other stability analysis technique, an appropriate value for the scaling factor, which ensures a good dynamic performance, can be designed. The feasibility of the suggested stability analysis has been verified by simulations with the MATLAB SIMULINK toolbox and experimentally using a digital signal processor (DSP TMS320F2808). As a future work this method will be investigated for its applicability to PV grid connected storage systems.

APPENDIX

The error signal (driving signal) is rewritten here as:

$$e = \frac{dv_{PV}}{di_{PV}} + \frac{v_{PV}}{i_{PV}} \tag{A1}$$

Linearizing e around (V_{mpp}, I_{mpp}) using the Taylor series expansion and neglecting the higher order terms leads to:

$$e = e(v_{PV}, i_{PV})|_{(V_{mpp}, I_{mpp})} + \left.\frac{\partial(v_{PV}, i_{PV})}{\partial v_{PV}}\right|_{(V_{mpp}, I_{mpp})} (v_{PV} - V_{mpp}) + \left.\frac{\partial(v_{PV}, i_{PV})}{\partial i_{PV}}\right|_{(V_{mpp}, I_{mpp})} (i_{PV} - I_{mpp}) \tag{A2}$$

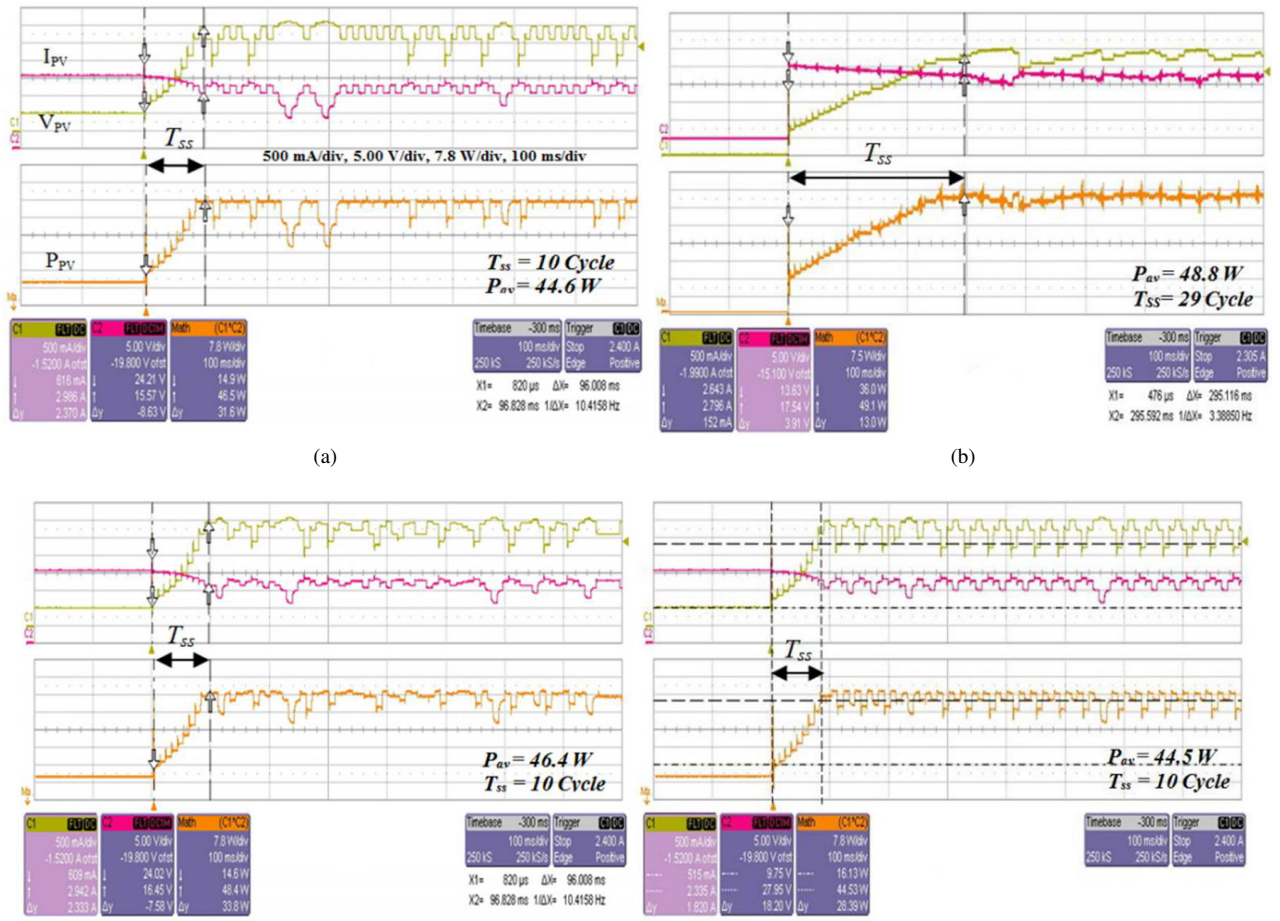

Fig. 11. Dynamic performance of the PV system with different scaling factors due to 1000 W/m^2 step change in the irradiation density (T_{ss} is the time to reach the steady state). (a) $\Delta D = 0.05$. (b) $N = 0.002I$ (c) $N = 0.01I$ (d) $N = 0.04I$.

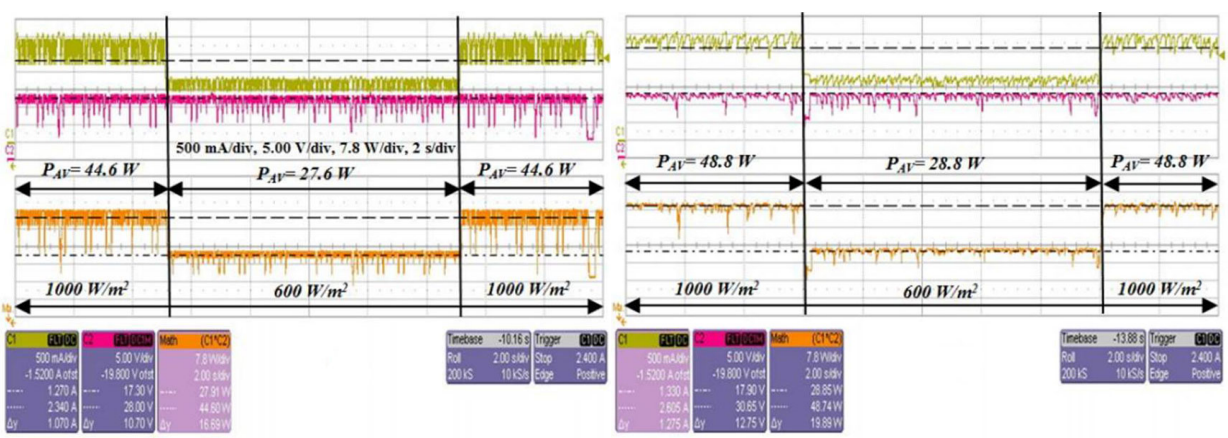

Fig. 12. Dynamic performance of the PV system with changing atmospheric condition from (1000 to 600 W/m^2) and back again. (a) Fixed step size $\Delta D = 0.05$ (b) Variable step size ($N = 0.002$).

Thus, by using (A1), the linearized equation becomes:

$$e = \left(\frac{dv_{PV}}{di_{PV}} + \frac{v_{PV}}{i_{PV}}\right)\Bigg|_{(V_{mpp},I_{mpp})} + \frac{1}{i_{PV}}\Bigg|_{(V_{mpp},I_{mpp})}(v_{PV} - V_{mpp}) + \frac{-v_{PV}}{i_{PV}^2}\Bigg|_{(V_{mpp},I_{mpp})}(i_{PV} - I_{mpp}) \tag{A3}$$

Substituting in (A3) and using (7) leads to:

$$e = (-R_{mpp} + R_{mpp}) + \frac{1}{I_{mpp}}(v_{PV} - V_{mpp}) + \frac{-V_{mpp}}{I_{mpp}^2}(i_{PV} - I_{mpp}) \tag{A4}$$

Substituting v_{PV} from (7), and using the fact that $R_{mpp} = V_{mpp}/I_{mpp}$

$$\Rightarrow \quad e = \frac{1}{I_{mpp}}(2V_{mpp} - i_{PV}R_{mpp} - V_{mpp}) + \frac{-V_{mpp}}{I_{mpp}^2}(i_{PV} - I_{mpp})$$

$$\Rightarrow\Rightarrow \qquad e = \frac{1}{I_{mpp}}(V_{mpp} - i_{PV}R_{mpp}) + \frac{-V_{mpp}}{I_{mpp}^2}(i_{PV} - I_{mpp})$$

$$\therefore \quad e = 2R_{mpp} - \left(\frac{R_{mpp}}{I_{mpp}} + \frac{V_{mpp}}{I_{mpp}^2}\right) i_{PV}$$

For further compression:

$$\Rightarrow e = 2R_{mpp} - \left(\frac{2R_{mpp}}{I_{mpp}}\right) i_{PV} \tag{A5}$$

Thus, the linearized actuating error variation around the MPP is written as:

$$\Rightarrow \Delta e = -\left(\frac{2R_{mpp}}{I_{mpp}}\right) \Delta i_{PV} \tag{A6}$$

REFERENCES

[1] H. Patel and V. Agarwal, "Maximum power point tracking scheme for pv systems operating under partially shaded conditions," *IEEE Trans. Ind. Electron.*, Vol. 55, No. 4, pp. 1689-1698, Apr. 2008.

[2] N. Femia, G. Lisi, G. Petrone, G. Spagnuolo, and M. Vitelli, "Distributed maximum power point tracking photovoltaic arrays: novel apprach and system analysis," *IEEE Trans. Ind. Electron.*, Vol. 55, No. 7, pp. 2610-2621, Jul. 2008.

[3] M. Veerachary, T. Senjyu, and K. Uezato, "Neural network based maximum power point tracking of coupled inductor interleaved boost converter supplied pv system using fuzzy controller," *IEEE Trans. Ind. Electron.*, Vol. 50, No. 4, pp. 749-758, Aug. 2003.

[4] N. D'Souza, L. Lopes, and X. Liu "Comparative study of variable step size perturbation and observation maximum power point trackers for PV systems," *Elec. Power Systs. Res.*, Vol. 80, pp. 296-305, 2010.

[5] K. H. Chao and C.-J. Li, "An intelligent maximum power point tracking method based on extension theory for PV Systems," *Expert Systems with Application*, Vol. 37, pp. 1050-1055, 2010.

[6] N. Femia, G. Petrone, and M. Vitelli, "Optimization of perturb and observe maximum power point tracking method," *IEEE Trans. Ind. Electron.*, vol. 20, no.4, pp. 963-973, Jul. 2005.

[7] K. H. Hussein, I. Muta, T. Hshino, and M. Osakada, "Maximum photovoltaic power tracking: an algorithm for rapidly changing atmospheric conditions," *In Proc. Inst. Elect. Eng.*, Vol. 142, No. 1, pp. 59-64, Jan. 1995.

[8] F. Liu, S. Duan, F. Liu, B. Liu, and Y. Kang, "A variable step size INC MPPT method for PV Systems," *IEEE Trans. Ind. Electron.*, Vol. 55, No.7, pp. 2622-2628, Jul. 2008.

[9] R. Kim, J. Lai, B. York, and A. Koran, "Analysis and design of maximum power point tracking scheme for thermoelectric battery energy storage system," *IEEE Trans. Ind. Electron.*, Vol. 56, No.9, pp. 3709-3716, Sep. 2009.

[10] E. M. Ahmed and M. Shoyama, "Variable step size maximum power point tracker using single variable for stand-alone battery storage pv system," *Journal of Power Electronics*, Vol. 11, No. 2, Mar. 2011.

[11] R. W. Erickson and D. Maksimovie, *Fundamental of Power Electronics*. Nerwell, MA: Kluwer, 2001

[12] E. M. Ahmed and M. Shoyama, "Modefied adaptive variable step size mppt based-on single current sensor," *in proceeding of TENCON-2010,* pp.1235-1240, 2010.

Emad M. Ahmed received his B.S. and M.S. in Electrical Engineering from South Valley University, Aswan, Egypt, in 2001 and 2006, respectively. He is currently working toward his Ph.D. in the Department of Electrical Engineering, Graduate School of Information Science and Electrical Engineering, Kyushu University, Fukuoka, Japan. Since 2002, he has been associated with the Department of Electrical Engineering, Faculty of Engineering, South Valley University, first as a Teaching Assistant and since 2006, as a Lecturer Assistant. His current research interests include power electronics, especially in renewable energy applications, artificial intelligence, and digital control. Mr. Ahmed received a Baek Hyun Award from the Korean Institute of Power Electronics (KIPE) for his academic contribution in the field of power electronics. He is a student member of IEEJ, IEEE Power Electronics Society (PELS), and IEEE Industrial Electronics Society (IES).

Masahito Shoyama received his B.S. in Electrical Engineering and his D.Eng. from Kyushu University, Fukuoka, Japan, in 1981 and 1986, respectively. He joined the Department of Electronics, Kyushu University as a Research Associate, in 1986, and became a Professor, in 2010. Since 1996, he has been with the Department of Electrical and Electronic Systems Engineering, Graduate School of Information Science and Electrical Engineering, Kyushu University. He has been active in the field of power electronics, especially in the areas of high-frequency switching power supplies, power factor correction, piezoelectric power converters, and electromagnetic compatibility (EMC). Dr. Shoyama is a member of IEEE, IEICE, IEEJ and SICE.